COMMUNICATION

Crystal surface defects as possible origins of cocrystal dissociation

Mark D. Eddleston,[a] Ernest H. H. Chow,[a] Dejan-Krešimir Bučar[b] and Ranjit Thakuria [a,c,*]

50Received 00th January 20xx,
Accepted 00th January 20xx

DOI: 10.1039/x0xx00000x

In situ **atomic force microscopy (AFM) was used to investigate topological crystal surface defects and their possible role in the dissociation of the caffine-glutaric acid cocrystal at high relative humidity (RH). Topographical scans of the cocrystal suggest that its decomposition is triggered by localized sublimation and involves increased molecular surface diffusion, the formation of line and screw dislocations and the crystallisation of caffeine hydrate.**

Cocrystallisation is now an established tool for the improvement of physicochemical properties of pharmaceuticals.[1] The growing interest in pharmaceutical cocrystals has prompted numerous studies that aim to better our understanding of their stability under processing and manufacturing conditions, whereby particular attention has been paid to excipients-cocrystal interactions[2-4] and the role of moisture and humidity in cocrystal dissociation.[5-9] Despite these recent efforts, and the recognition that crystal defects possibly play a significant role in the cocrystal dissociation process,[5, 10, 11] little is known about the mechanistic aspects of such dissociation. We also note that no investigations have so far interrogated the mechanisms of cocrystal dissociation on a molecular level, and argue that knowledge derived from such studies could guide the optimisation of cocrystal manufacturing and processing.

Our previous efforts to understand the impact of humidity on cocrystal stability,[8] and how atomic force microscopy (AFM) can be used to understand phase transformations of cocrystals,[12] have recently inspired a pursuit for more evidence that intrinsic crystal defects (such as line, edge and screw dislocations)[13] play an active role in the dissociation of cocrystals. We now report how *in situ* intermittent contact mode-AFM (IC-AFM) was used to visually identify topological crystal defects as sites around which cocrystal dissociation occurs. The object of our study was the polymorphic 1:1 caffeine:glutaric acid cocrystal[14] for which we have shown in earlier work[10, 12, 15] that its Form I transforms to Form II at high relative humidity (RH), followed by cocrystal dissociation through deliquescence of glutaric acid and the recrystallization of caffeine hydrate. These studies have also suggested that defects, induced during its mechanochemical formation, render the cocrystal more susceptible to dissociation in humid conditions, which prompted us to monitor these defects using IC-AFM to determine their role in the dissociation process.

We report here the results of a more recent AFM analyses of the molecularly flat (001) crystal faces in the two polymorphs, which is dominant in each form. These studies have led to the observation of dislocation sites on the surfaces of freshly cleaved single crystals of Form II, while such features were absent on the surface of the investigated single crystals of Form I. We have also observed that the cocrystal dissociation is associated with the development of rectangular grooves (Figure 2a) and propose that a variety of variety of events on the cocrystal surface facilitate the decomposition of Form II. These include sublimation, water-induced surface etching, and the diffusion of caffeine and glutaric acid molecules along the cocrystal surface. The cocrystal dissociation evidenced by the formation of needle shaped crystals, which were in an earlier related study identified as caffeine hydrate.[15]

The rates of cocrystal dissociation were determined using sublimation rates (at 0% relative humidity, RH), and rates at which a possible combination of water etching and sublimation (at 40% and 70% RH) lead to the disappearance of molecular cocrystal layers. The rates were calculated by measuring the distances between the opposite faces of the growing grooves on the cocrystal surface as a function of time. The two measured distances between monitored crystal surface features run parallel to the (141) crystal plan (henceforth

[a] *Yusuf Hamied Department of Chemistry, University of Cambridge, Lensfield Road, Cambridge CB2 1EW, United Kingdom.*
[b] *Department of Chemistry, University College London, 20 Gordon Street, London WC1H 0AJ, United Kingdom.*
[c] *Department of Chemistry, Gauhati University, Guwahati 781014, India. E-mail: ranjit.thakuria@gauhati.ac.in.*

† Footnotes relating to the title and/or authors should appear here.
Electronic Supplementary Information (ESI) available: IC-AFM images and videos of caffeine-glutaric acid Form II under various humidity and excel plots of groove boundary (nm) vs. time (sec.). See DOI: 10.1039/x0xx00000x

Deleted: dissociation
Deleted: possibly
Deleted: ,
Deleted: ,
Deleted: the
Deleted: and, finally,
Deleted: 10, 12, 15
Deleted: Our
Deleted: ,
Deleted: preceded
Deleted: by
Deleted:
Deleted: of the coformerscocrystal
Deleted: , followed by surface diffusion
Deleted: This was implied by the formation of rectangular grooves (Figure 2a) and the
Deleted: sublimation
Deleted: used to quantify the dissociation events
Deleted: These

referred to as 'short axis') and parallel to (101) crystal plan (hereafter referred to as 'long axis'). The crystallographic planes of interest and their relative orientation to the caffeine and glutaric acid molecules in Form II are shown in Figure 1.

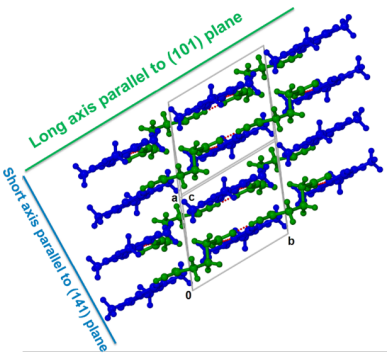

Figure 1. Internal arrangement of caffeine-glutaric acid molecules viewed under identical orientation as that of the rectangular groove along the long and short axis. Colour scheme: blue – caffeine, green – glutaric acid.

A series of IC-AFM analyses of the (001) crystal face of caffeine-glutaric acid cocrystal Form II was conducted at ambient temperature and under controlled relative humidity (RH) to investigate the role of crystal surface defects in the dissociation of Form II. Our observations, including the formation and the development of the surface grooves, are described below.

Surface diffusion events at 0% RH. IC-AFM height images of a cleaved single crystal of Form II, matured for 12 days at 0% RH, showed well-defined screw and edge dislocations. The screw dislocation sites appeared to act as the origin of sublimation, followed by increased surface diffusion events, which resulted in the formation of rectangular grooves. Figures 2 shows the surface groove, resembling a right-handed screw that formed through local sublimation (at 0% RH), and highlight the increase in groove size using blue coloured broken lines. The rate of sublimation was monitored by plotting the short and long axial distances over time. The sublimation rate was calculated using the AFM image scan rate. For details see the experimental section, Figure S1 and Movie S1 in the Electronic Supporting Information (ESI) document. The sublimation along the long axis was found to be faster (0.25 nm s^{-1}) than along the short axis (0.14 nm s^{-1}), thus highlighting the anisotropic nature of the sublimation across the groove boundary. The upper side of the rectangular groove, situated beneath the molecular layers, did not show any signs of sublimation during the experiment.

The edge dislocations moved diagonally across the groove and finally receded through the upper left side of the groove, as shown in Figure 3.

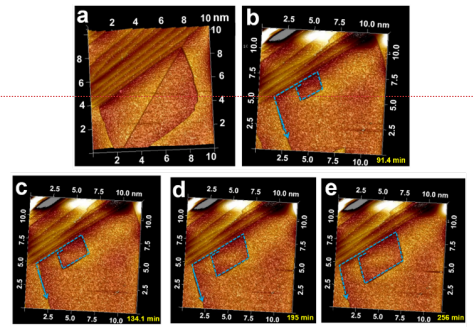

Figure 2. IC-AFM images showing: (a) a rectangular groove formed through sublimation and molecular diffusion, (b-e) the evolution of the groove (resembling a right-handed screw) over a 2.5-hour period. The increase of the groove size is highlighted using a blue arrow.

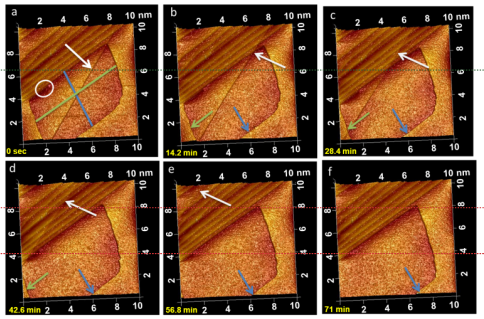

Figure 3. IC-AFM height images of Form II under 0% RH after 12 days. Screw dislocation defects that induce molecular diffusion are observed as the rectangular groove increases with time (see ESI Movie S1). (a) Screw and edge dislocations are highlighted with white circles and arrows, respectively. The short and long groove axes are highlighted using blue and green colored solid line. The increase in groove boundary is emphasised using the blue (b-f) and green arrows (b-d).

Surface diffusion events at 40% RH. The formation of screw dislocation defects was observed at 40% RH conditions (Area 1, Figure S2 and Movie S2 in ESI). Similar to the crystal studied at 0% RH, we have observed an anisotropy in the groove development across the short and long axis. The rate of sublimation (possibly assisted by water etching) was found to be 1.6 times faster along the long axis (0.13 nm s^{-1}), as compared to the short axis (0.08 nm s^{-1}) across the groove boundary (see ESI Figure S3). Although there were no stacks of layers situated over the upper side of the rectangular groove, the upper boundary remained unchanged during the sublimation event.

Deleted: Figures 2b-e show the groove, resembling a right-handed screw, which formed through local sublimation, and highlight the increase in groove size using blue coloured broken lines....
Deleted: ¶
Moved up [1]: **Figure 1.** Internal arrangement of caffeine-glutaric acid molecules viewed under identical orientation as
Deleted: ¶ ... [2]
Deleted: the evolution of
Deleted: during
Deleted: sublimation followed by surface diffusion show ... [3]
Deleted: direction of molecular diffusion (right-handed ... [4]
Deleted: in
Deleted: as a function of time
Deleted: shown
Deleted: coloured broken lines
Moved (insertion) [1]
Deleted:
Deleted: whether
Deleted: play a role
Deleted: ¶
Deleted: inducing
Deleted: can be
Deleted: as a function of
Deleted: represented
Deleted: by
Deleted: cursor
Deleted: Short
Deleted: represented
Deleted: by
Deleted: ,
Deleted: shown
Deleted: by
Deleted: cursor
Deleted: The edge dislocations moved diagonally across ... [1]
Deleted: (
Deleted: can be
Deleted: based on
Deleted: sublimation
Deleted: ;
Deleted: see ESI E
Deleted: section
Deleted: , Figure S1 and Movie S1)
Deleted: proceed
Deleted: investigation period
Formatted: Space Before: 0 pt

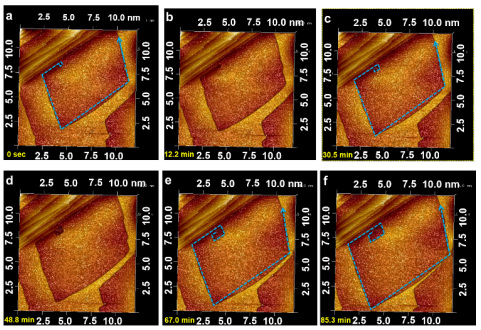

Figure 4. IC-AFM height images of Form II (Area 2) recorded at 40% humidity. Screw dislocation inducing molecular diffusion can be observed as the rectangular groove across the surface (see ESI Movie S3). The direction of molecular sublimation (right-handed screw) and the increase in groove size over a 1.5-hour period is highlighted using a blue arrow.

Screw dislocation sites and evidence of sublimation and surface diffusion were also observed in another area (Area 2) on the same crystal surface (Figure 4 and Movie S3 in ESI). The rates of the sublimation along the long and short axes were found to be 0.32 nm s^{-1} and 0.18 nm s^{-1}, respectively (Figure 5).

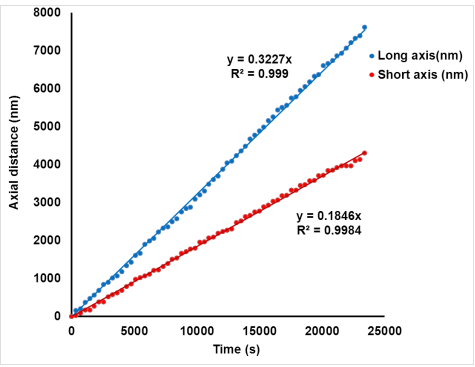

Figure 5. Change in axial distances (shown as a function of time) during sublimation across the four faces with different rate (Area 2) at 40% humidity.

The investigation of a third area (Area 3) of the cocrystal surface revealed the appearance of surface deposits, which are presumably locations of new crystal growth. Time-resolved IC-AFM height images also revealed the presence of screw dislocations in the vicinity of these deposits, while edge dislocations were observed across the upper left side of the crystal surface (Figure 6 and Movie S4 in ESI). We further found that all screw dislocations formed by local sublimation (or, again, by a combination of sublimation and water etching) were right-handed, while the only observed screw dislocation formed through crystal growth was left-handed. This observation is consistent with the results of an earlier study of crystal dissolution kinetics, which demonstrated that the *'handedness of the dissolution spirals is opposite to that found for steps in growth spirals'*.[16] It is not clear, at this point, why all observed sublimation screw dislocations in our study were right-handed.

We note that numerous sublimation and etching events were observed in the entire investigated area of the cocrystal face, while only one crystal growth site was spotted. The rates of the anisotropic crystal growth across the long and short axes were significantly higher (2.62 nm s^{-1} and 1.76 nm s^{-1}, respectively) than the observed sublimation rates (see ESI Figure S4).

Figure 6. IC-AFM height images of Form II (Area 3) at 40% RH. Screw-dislocation-induced crystal growth is highlighted with the blue arrow, while edge dislocations are highlighted with the white arrows. The dashed green arrows indicate the clockwise direction of crystal growth (see ESI Movie S4). The growth is facilitated by fresh cocrystal surface deposition (as previously evidenced by AFM height images[12]) along the investigated surface.

Surface diffusion events at 70% RH. Two dislocation sites were found in Area 4 at 70% RH and seem to act as the origin of cocrystal sublimation, water etching or a combination of both events (Figure 7 and Figure S5). By measuring sublimation/etching rates over the rectangular grooves (upper and lower sides) across the crystal surface (see ESI Figure S6), it was determined that the grove development (and thus cocrystal dissociation) at 70% RH is 0.92 nm s^{-1} and 0.46 nm s^{-1} along the long and short axes, respectively. The ESI Movie S5 and Figure S7-S9 highlight the interplay of local sublimation and cocrystal deposition. The rates of the groove development increase with an increase of the relative humidity in the atmosphere (Figure 8).

Deleted: study that

Deleted:

Formatted: Indent: First line: 0 cm

Deleted: under

Deleted: humidity

Deleted: Screw

Deleted: under

Commented [BK1]: I don't understand it. Something is missing.

Deleted: Direction

Deleted: right

Deleted: w.r.t. time of scan is

Deleted: shown

Deleted: coloured broken lines

Deleted: , followed by

Deleted: ,

Deleted: dislocation

Deleted: are

Deleted: whereas

Deleted: (Area 4)

Deleted: that

Deleted: rate of sublimation

Commented [BK2]: Please remove the grey box around the graph.

Deleted: (t

Deleted: show

Deleted:)

Deleted: An increase in the rate of sublimation was observed at with an

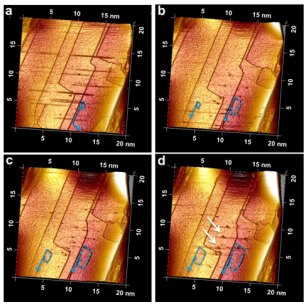

Figure 7. IC-AFM height images of Form II at 70% RH show two screw dislocation sites, highlighted using blue arrows (see ESI Movie S5). The white protrusions observed in image (d), highlighted using white arrows, correspond to newly formed caffeine hydrate needles on the cocrystal surface confirmed based on our previous reports[10, 15].

A crystallographic face indexing exercise of the studied single crystals revealed that infinite chains of hydrogen-bonded caffeine-glutaric acid assemblies are oriented parallel to the long axis of the grove, and that these are stacked along the direction of the short grove axis (Figure 1a). The crystallographic *c* axis runs normal to the plane of the rectangular groove and is aligned with the tilted stacks of the caffeine:glutaric acid molecular tapes.[12] IC-AFM studies and earlier reported X-ray diffraction analyses[10] show that the direction of the observed anisotropic molecular sublimation along the surface, and that of the cocrystal deposition (growth), corresponds to the direction of the hydrogen-bonded chains composed of caffeine and glutaric acid. The sublimation, water etching and crystal deposition events were found to proceed at significantly higher rates along the long axis of the groove, as compared to the rate of the same events along the short axis and in the direction of the stacked caffeine:glutaric acid chains. All sublimation, water etching, diffusion and surface deposition processes seem to originate in the vicinity of screw dislocation sites, while the disappearance of the cocrystal surface layers (either through sublimation or water etching) and the growth of new crystalline surface deposits occur with opposite handiness.

Our observations suggest that the cocrystal decomposes even at low rates at 0% RH through sublimation, as evidenced by the formation of surface grooves. The number of sublimation sites and the sublimation rates increase with an increase in RH. We propose that the observed sublimation of caffeine and glutaric acid molecules at 40% and 70% is facilitated by atmospheric water through surface etching.[17-20] The atmospheric water also contributes to the deliquescence of glutaric acid and the formation of caffeine hydrate (in form of needles) crystals on the investigated surface (Figure 7d, ESI Figure S5f and Movie S5). Our study also implies that the caffeine-glutaric acid cocrystal dissociation and re-growth are in equilibrium and are relatively slow under low humid conditions. We speculate that the cocrystal re-growth occurs either when gaseous molecules of caffeine and glutaric acid (which both linger above the crystal surface because of localized sublimation and surface diffusion events) interact with each other, or through a recrystallisation of from surface regions rich in water.

In conclusion, we used *in situ* IC-AFM height images to observe the dissociation of Form II of the caffeine-glutaric acid cocrystal at high RH, and to identify screw dislocations as origins of the cocrystal dissociation. Our findings are not only underpinning the previously speculated importance of crystal structure defects to the process of cocrystal dissociation,[10] but also show that cocrystal dissociation under humid conditions is seemingly accompanied by sublimation, surface diffusion and recrystallisation events. Our study is also underpinning the importance and usefulness of AFM (and other microscopy)[21, 22] techniques in mechanistic studies of solid state transformations, in establishing structure-mechanical property relationships and in organic solid-state in general.[23-34] We are now investigating how different cocrystallisation methods (*e.g.* milling and solution-based methods) affect the dissociation rates of water sensitive cocrystals at high relative humidity, and hope that these efforts will in the future aid the development and manufacturing of medicines involving moisture sensitive cocrystals.

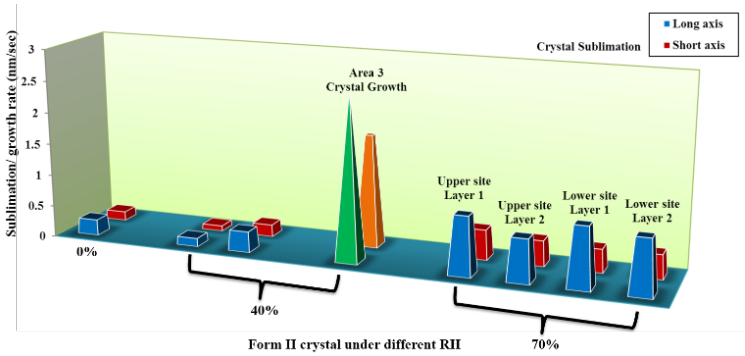

Figure 8. Rate of sublimation/deposition (nm s^{-1}) of Form II cocrystal under studied humidity conditions is shown as a bar diagram. Different crystal areas were selected to measure the size of rectangular groove observed during sublimation/ deposition.

Deleted: n
Deleted: cocrystal
Moved (insertion) [2]
Deleted: We also note that t
Deleted: ,
Deleted: as well as
Deleted: ,
Deleted: s
Deleted: resulting cocrystal dissociation
Deleted: dissociates through a reaction of the caffeine and glutaric acid molecules on the crystal surface with atmospheric water, which possibly acts as etchant
Deleted: surface etching then
Deleted: results in
Deleted: , which is followed by
Deleted: recrystallization
Deleted: ¶
Deleted: under
Deleted: with
Deleted: the
Deleted:
Deleted: using the two
Deleted: ,
Deleted: ,
Moved up [2]: We also note that the number of sublimation sites, as well as the sublimation rate, increases with an increase in RH resulting cocrystal dissociation.
Deleted: .
Deleted: ¶
Commented [BK3]: insert references of: Kaupp (under other microscopy techniques), Mike Ward, Mall Reddy, Desiraju, Venu (and Bradford crew), Aurora and others. Please do not use less than 8 references! Go crazy and show at least ten. Also, add Ernest's review (he's an author and will appreciate it). Be diplomatic.
Commented [BK4]: Please order these references chronologically.
Deleted: molecular
Deleted: based on
Deleted: sublimatio
Deleted: ¶
¶
Deleted:

R.T. and E.H.H.C. are grateful to the Pfizer Institute for Pharmaceutical Materials Science and M.D.E. to the EU INTERREG IVA 2 Mers Seas Zeeën Cross-border Cooperation Programme for financial support. We would also like to thank Prof. William Jones of the Yusuf Hamied Department of Chemistry at the University of Cambridge for support.

Notes and references

1. O. N. Kavanagh, D. M. Croker, G. M. Walker and M. J. Zaworotko, *Drug Discov. Today*, 2019, **24**, 796-804.
2. M. Aljohani, P. McArdle and A. Erxleben, *Cryst. Growth Des.*, 2020, **20**, 4523-4532.
3. N. K. Duggirala, A. Vyas, J. F. Krzyzaniak, K. K. Arora and R. Suryanarayanan, *Mol. Pharmaceutics*, 2017, **14**, 3879-3887.
4. S. Koranne, J. F. Krzyzaniak, S. Luthra, K. K. Arora and R. Suryanarayanan, *Cryst. Growth Des.*, 2019, **19**, 868-875.
5. N. Kaur, N. K. Duggirala, S. Thakral and R. Suryanarayanan, *Mol. Pharmaceutics*, 2019, **16**, 3167-3177.
6. S. Koranne, A. Sahoo, J. F. Krzyzaniak, S. Luthra, K. K. Arora and R. Suryanarayanan, *Mol. Pharmaceutics*, 2018, **15**, 3297-3307.
7. H. Veith, M. Zaeh, C. Luebbert, N. Rodríguez-Hornedo and G. Sadowski, *Pharmaceutics*, 2021, **13**, 433.
8. M. D. Eddleston, R. Thakuria, B. J. Aldous and W. Jones, *J. Pharm. Sci.*, 2014, **103**, 2859-2864.
9. M. D. Eddleston, N. Madusanka and W. Jones, *J. Pharm. Sci.*, 2014, **103**, 2865-2870.
10. R. Thakuria, M. Arhangelskis, M. D. Eddleston, E. H. H. Chow, K. K. Sarmah, B. J. Aldous, J. F. Krzyzaniak and W. Jones, *Org. Process Res. Dev.*, 2019, **23**, 845-851.
11. G. Schneider-Rauber, M. Arhangelskis, W.-P. Goh, J. Cattle, N. Hondow, R. Drummond-Brydson, M. Ghadiri, K. Sinha, R. Ho, N. K. Nere, S. Bordawekar, A. Y. Sheikh and W. Jones, *Chem. Sci.*, 2021, **12**, 14270-14280.
12. R. Thakuria, M. D. Eddleston, E. H. H. Chow, G. O. Lloyd, B. J. Aldous, J. F. Krzyzaniak, A. D. Bond and W. Jones, *Angew. Chem., Int. Ed.*, 2013, **52**, 10541-10544.
13. A. M. Stoneham, *Theory of Defects in Solids: Electronic Structure of Defects in Insulators and Semiconductors*, Clarendon Press, 1985.
14. A. V. Trask, W. D. S. Motherwell and W. Jones, *Chem. Commun.*, 2004, 890-891.
15. R. Thakuria, M. D. Eddleston, E. H. H. Chow, L. J. Taylor, B. J. Aldous, J. F. Krzyzaniak and W. Jones, *CrystEngComm*, 2016, **18**, 5296-5301.
16. M. Adobes-Vidal, A. G. Shtukenberg, M. D. Ward and P. R. Unwin, *Cryst. Growth Des.*, 2017, **17**, 1766-1774.
17. H. M. Burt and A. G. Mitchell, *Int. J. Pharm.*, 1981, **9**, 137-152.
18. K. Sangwal, *Etching of crystals: theory, experiment and application*, Elsevier, 2012.
19. J. Thomas, G. Renshaw and C. Roscoe, *Nature*, 1964, **203**, 72-73.
20. R. E. Keith and J. J. Gilman, *Acta Metallurgica*, 1960, **8**, 1-10.
21. G. Kaupp and M. R. Naimi-Jamal, *CrystEngComm*, 2005, **7**, 402-410.
22. G. Kaupp, J. Schmeyers and U. D. Hangen, *J. Phys. Org. Chem.*, 2002, **15**, 307-313.
23. L. N. Poloni, X. Zhong, M. D. Ward and T. Mandal, *Chem. Mater.*, 2017, **29**, 331-345.
24. M. D. Ward, *Science*, 2005, **308**, 1566-1567.
25. D. Musumeci and M. D. Ward, *CrystEngComm*, 2011, **13**, 1067-1069.
26. A. G. Shtukenberg, M. D. Ward and B. Kahr, *Chem. Rev.*, 2017, **117**, 14042-14090.
27. M. S. R. N. Kiran, S. Varughese, C. M. Reddy, U. Ramamurty and G. R. Desiraju, *Cryst. Growth Des.*, 2010, **10**, 4650-4655.
28. M. K. Mishra, K. Mishra, A. Narayan, C. M. Reddy and V. R. Vangala, *Cryst. Growth Des.*, 2020, **20**, 6306-6315.
29. S. Varughese, M. S. R. N. Kiran, U. Ramamurty and G. R. Desiraju, *Angew. Chem., Int. Ed.*, 2013, **52**, 2701-2712.
30. M. B. Alsirawan, X. Lai, R. Prohens, V. R. Vangala, S. K. Pagire, P. Shelley, T. J. Bannan, D. O. Topping and A. Paradkar, *Cryst. Growth Des.*, 2020, **20**, 7598-7605.
31. E. H. H. Chow, D.-K. Bucar and W. Jones, *Chem. Commun.*, 2012, **48**, 9210-9226.
32. R. Montis, R. J. Davey, S. E. Wright, G. R. Woollam and A. J. Cruz-Cabeza, *Angew. Chem., Int. Ed.*, 2020, **59**, 20357-20360.
33. B. P. A. Gabriele, C. J. Williams, M. E. Lauer, B. Derby and A. J. Cruz-Cabeza, *Cryst. Growth Des.*, 2020, **20**, 5956-5966.
34. B. P. A. Gabriele, C. J. Williams, D. Stauffer, B. Derby and A. J. Cruz-Cabeza, *Cryst. Growth Des.*, 2021, **21**, 1786-1790.

Deleted: ,

Deleted: ,

Page 2: [1] Deleted Bucar, Kreso 09/05/2022 15:12:00

Page 2: [2] Deleted Bucar, Kreso 09/05/2022 15:13:00

Page 2: [3] Deleted Bucar, Kreso 09/05/2022 10:37:00

Page 2: [4] Deleted Bucar, Kreso 09/05/2022 10:42:00